Aggregation of Rare Earth Coordination Complexes in Solution Studied by Paramagnetic and DOSY NMR

Adeline W. J. Poh, Juan A. Aguilar, Alan M. Kenwright, Kevin Mason and David Parker*

Department of Chemistry, Durham University, South Road, Durham. DH1 3LE, UK

E-mail: ***david.parker@dur.ac.uk*** Supporting information and ORCID(s) from the author(s) for this article are available on the www under ***http://dx.doi.org/10.1002/chem.***xxxxx

Abstract

The degree of aggregation of neutral, 9-coordinate rare earth coordination complexes has been shown to affect their ligand field, as revealed by DOSY-NMR measurements on Y(III) complexes, paramagnetic NMR analyses of Yb and Tb analogues and emission spectral studies with the Eu(III) systems. In non-polar media a lipophilic tris-isopropyl complex, [Ln.L^2] tends to aggregate in chloroform and dichloromethane giving rise to oligomers, whilst in acetic and trifluoroacetic acid the more polar parent complex, [Ln.L^1] also aggregates, profoundly affecting the pseudocontact shift and the form of the Eu emission spectrum. Such behaviour has important implications in the design of responsive spectral probes.

Introduction

Studies of lanthanide coordination complexes continue to attract attention owing to their utility as spectroscopic probes in a wide range of chemical, biological and clinical applications. [1-5] Detailed NMR and emission spectral analyses of closely related series of paramagnetic lanthanide coordination complexes have pinpointed the sensitivity of the ligand field to changes in the second coordination sphere, arising from medium polarity effects. [6,7] In polar, protic media, evidence has been found for specific solvent interactions, linked to hydrogen bonding interactions involving those ligand carboxylate oxygen atoms that are bound to the lanthanide ion. In a series of complexes based on nonadentate *tris*(pyridylcarboxylate)-1,4,7-

triazacyclononane ligands, [Ln.L^n], the solvent polarity determines the pseudocontact shift (PCS) of the ligand ^{1}H NMR resonances. Such behaviour was attributed to solvent dipolar fluctuations that modulate the Ln-O and Ln-N_{py} dipolar and quadrupolar interactions. Such ideas of a key solvent effect can be traced back to earlier theoretical work. [8-10] There are clear implications for the design and analysis of lanthanide probes when the distinct sensitivity of the ligand field is considered. Only by gaining a good understanding of the solution dynamics and local magnetic susceptibility can pseudocontact shift data be used in probe design with confidence, e.g. in detailed structural analyses.

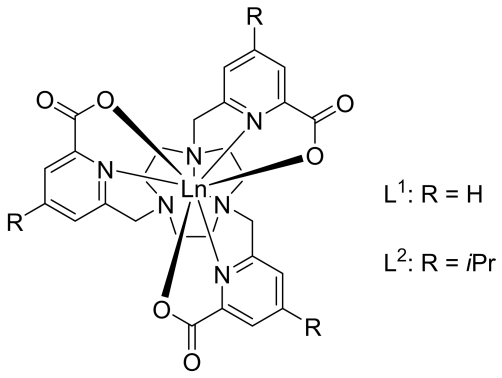

Scheme 1 Molecular structure of [Ln.L$^{1-2}$]; proton labelling scheme, see Figure S1.

Amongst this series of complexes, the complex, [Yb.L^2] was introduced as a paramagnetic chemical shift probe for solvent polarity. The chemical shift separation of the peripheral isopropyl methyl groups was used as the measurable parameter , obviating issues of calibration. [7] This work delves into the behaviour of these molecules in non-polar and very polar (acidic) media, in an attempt to define the scope and limitations of such systems as spectral probes.

Results and Discussion

Solution Behaviour of [Ln.L^2]

The introduction of the isopropyl substituent in the *para*-position of the pyridine ring substantially enhances the solubility of [Ln.L^2], (Ln = Y, Tb, Yb and Eu) in non-polar media. It was therefore possible to perform detailed NMR analyses of these C_3-symmetric tricarboxylate systems in a wider range of solvents. Earlier work with [Yb.L^1] had been restricted by solubility issues to DMSO, methanol and water.

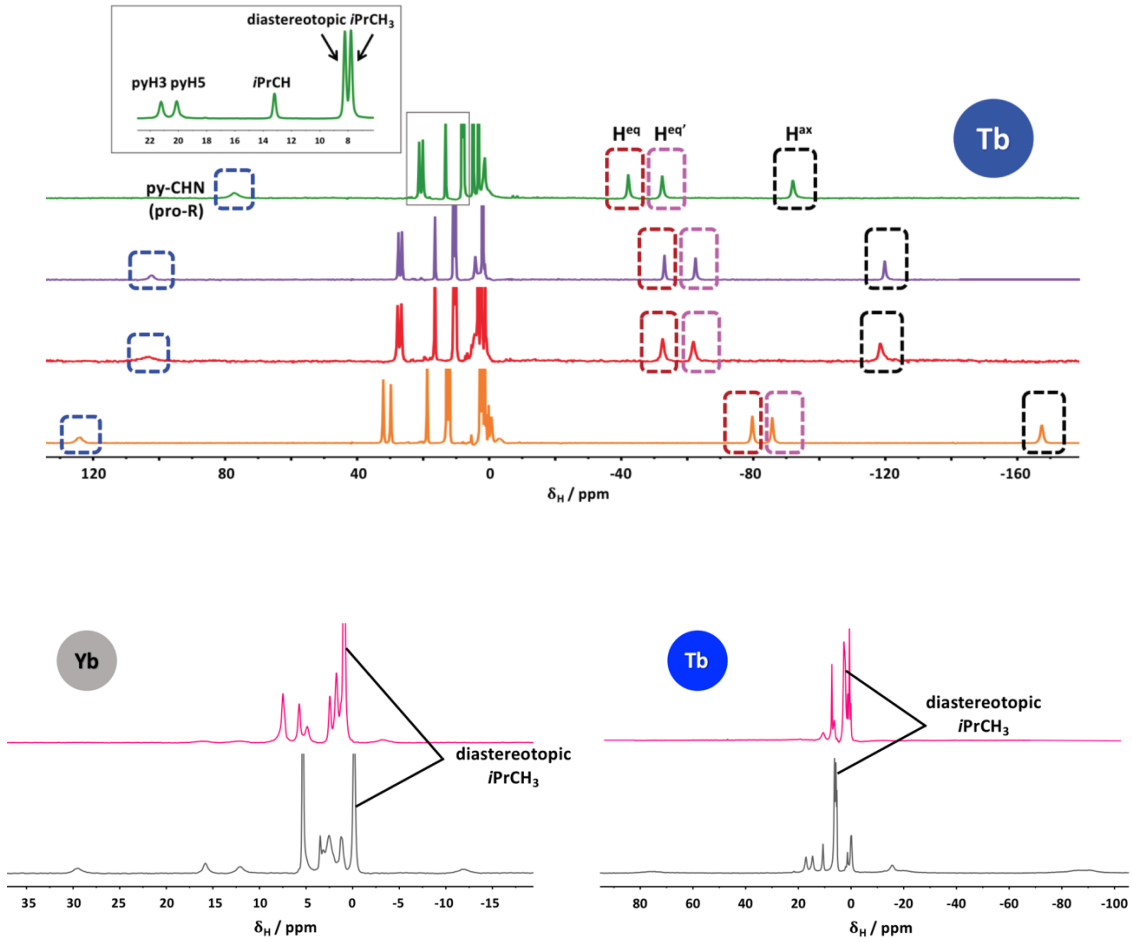

Fig. 1 (*upper*): ^{1}H NMR spectra of [TbL^{2}] in MeOD (green), MeCN-d_3 (purple), DMSO-d_6 (red) and acetone-d_6 (orange) (4.7 T, 295 K). (*lower*) Annotated ^{1}H NMR spectra of [Yb.L^{2}] (*left*) and [Tb.L^{2}] (*right*) in $CDCl_3$ (*top)* and CD_2Cl_2 (4.7 T, 295 K), showing the rather broad paramagnetically shifted resonances.

The ^{1}H NMR spectra of [Yb.L^{2}] and [Tb.L^{2}] in $CDCl_3$ and CD_2Cl_2 showed rather severe line broadening and the overlapping of some resonances. Such behaviour was quite different in the spectra of solutions in d^{6}-DMSO or CD_3OD (*Fig. 1 (upper), Yb spectra Figure S2*). In $CDCl_3$ particularly, the most shifted resonances almost disappeared into the baseline. In each case, the diastereotopic methyl group signals were not resolved but appeared as a rather broad, single resonance. Difficulties in measuring and comparing the relaxation rates against the geometric coordinates found from the X-ray crystallographic structure[7] made it impossible to assign with confidence most ligand proton resonances. Variable temperature (VT) NMR studies were carried out, seeking to investigate the origin of the observed line broadening. If the methyl groups were in fast exchange on the NMR timescale, then low temperature experiments might resolve these resonances, as they enter the slow exchange regime. However, no such signal resolution was observed, even

at 183 K, suggesting that a chemical exchange process was not responsible for the broadening of the complex resonances. Increased broadening can also be caused by any form of organisation in which the resulting entity grows in size; aggregation is one possibility, although other forms of self-organization are also possible. We first saw indications of some of these effects while analysing the NOESY spectra (Figure S3). For molecules rotating quickly with respect to the Larmor frequency, the nuclear Overhauser (nOe) effect should be positive, thereby leading to signals with the opposite phase to the diagonal; this was observed for [Y.L^2] dissolved in CD_3OD. However, these signals become positive (i.e., a negative nOe) when the rotation is slower than the Larmor frequency, as was the case for [Y.L^2] dissolved in $CDCl_3$. Such changes can also be attributed to differences in solvent viscosity. However, the viscosities of these solvents are very similar (MeOD: 0.61 x 10^{-3} kg m^{-1} s^{-1} and $CDCl_3$: 0.54 x 10^{-3} kg m^{-1} s^{-1}), indicating that the size of the entity present in solution has a mass that depends on the nature of the solvent used, not its viscosity.

We therefore resorted to diffusion-ordered spectroscopy (DOSY-NMR) as a more accurate means of investigating whether the molecules in solution were aggregating or self-organising. [11,12] Using these experiments, it is possible to estimate the diffusion coefficient, and with the aid of Eq. 1, [13] the molecular mass of species in solution can be estimated,

$$D = \frac{k_B T\left(\frac{3\alpha}{2}+\frac{1}{1+\alpha}\right)}{6\pi\eta\sqrt[3]{\frac{3MW}{4\pi\rho_{eff}N_A}}}, \text{ where } \alpha = \sqrt[3]{\frac{MW_s}{MW}} \quad (1)$$

where MW and MW_s are the solute and solvent molecular weight respectively, η is the viscosity of the solvent and ρ_{eff} is an empirical parameter which sets the effective density of a small molecule as 619 kg m^{-3}, based on a collection of experimental data.

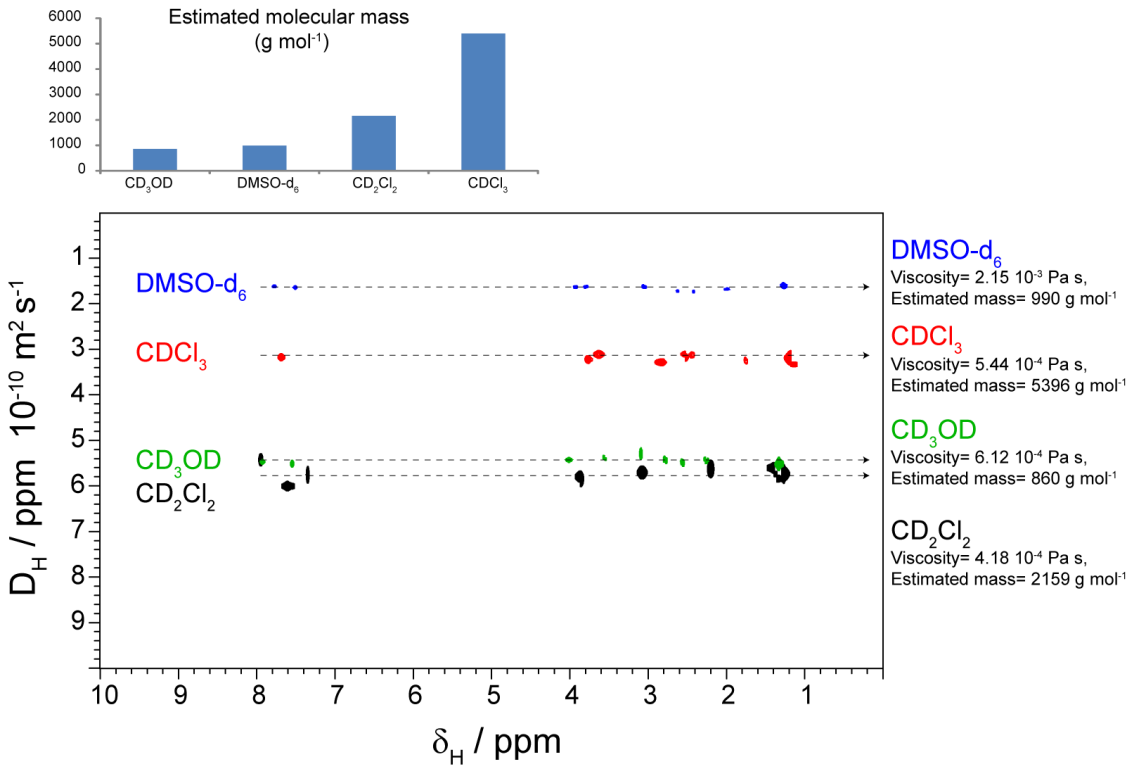

Fig. 2 Stacked DOSY representation of [YL^2] in $CDCl_3$ (*red*), DMSO-d_6 (*blue*), DCM-d_2 (*black*) and CD_3OD (*green*) (14.1 T, 298 K) with solvent viscosity and the estimated molecular weight, MW_{est}, of [$Y.L^2$] in each solution found from the experimental diffusion coefficient, *D* (dotted line) using an Excel spreadsheet made available by Morris et al. [13].

Table 1 Estimated molecular mass of [Y.L^2] in different solvents and the normalised ratio with respect to the lowest figure.

Solvent	MW_{est} / g mol^{-1}	Ratio
CD_3OD	860	1.0
$(CD_3)_2SO$	990	1.2
CD_2Cl_2	2159	2.5
$CDCl_3$	5396	6.3

Some deviations to this ideal behaviour are expected in cases such as the present one, where heavy atoms are present. Notwithstanding such deviations, it is clear from the experimental data (Figure 2) that [Y.L^2] is aggregating or self-organising, (Table 1). For example, the estimated mass in CD_2Cl_2 is twice as large as the estimated mass in CD_3OD or DMSO-d_6, and it is more than six times larger in $CDCl_3$. This direct evidence for aggregation of the complex is perhaps unsurprising in such non-polar solvents, as solvation of the complex via intermolecular induced dipole interactions is weak and allows both CH- π and hydrophobic π- π stacking to occur between the aromatic rings. A comparison between the values of the estimated molecular weights implies that aggregation is more significant in $CDCl_3$ than in CD_2Cl_2; indeed, $CDCl_3$ is the more non-polar solvent. Such an analysis rationalises the severity of the line broadening in the NMR spectra of [Yb.L^2] and [Tb.L^4] in $CDCl_3$, associated with intermolecular chemical exchange between monomers and oligomers, and the resultant rather slow rate of molecular tumbling.

Solvent effects in the emission of [EuL^2]

Emission studies examining [Eu.L^2] in varying solvents focused on the analysis of the $\Delta J = 1$ emission band around 590 nm. [4,5] Owing to the time-averaged C_3 symmetry of the [Eu.L^2] complexes, the splitting of the ground state $^7F_1$ level was used to confirm independently the effect of solvent polarity on the electronic structure of the Ln(III) complex. The sign of B_0^2 is negative in all solvents. [14] In polar solvents, the separation between the singlet and doublet energy levels decreases as the solvent varies from DMSO to MeCN to MeOH to H_2O.. Since the pseudocontact shift (PCS) is directly proportional to B_0^2, the overall crystal field

splitting and observed NMR shift range should be comparable. Similar values of B_0^2 in DMSO and MeCN were found, consistent with the absence of significant differences in the NMR spectral width of the Yb(III) and Tb(III) analogues in each of these solvents (Fig. 3). The Reichardt solvent polarity parameter [15] varies very little between DMSO and MeCN (E_T = 0.444 and 0.460 respectively). Hence, it was hypothesised that these two solvents induce similar changes in the electromagnetic susceptibility anisotropy of the lanthanide complex.

An interesting observation was made regarding the spectral form of the complex in $CHCl_3$ and, to a lesser extent, in CH_2Cl_2. The appearance of a shoulder at approximately 588 nm suggests that the complex is not perfectly C_3-symmetric in non-polar solvents. This observation is perhaps unsurprising, given the evidence for species aggregation from DOSY experiments, and can tentatively rationalise the breakdown of time-averaged C_3 symmetry in [EuL^2], (Fig. 3).

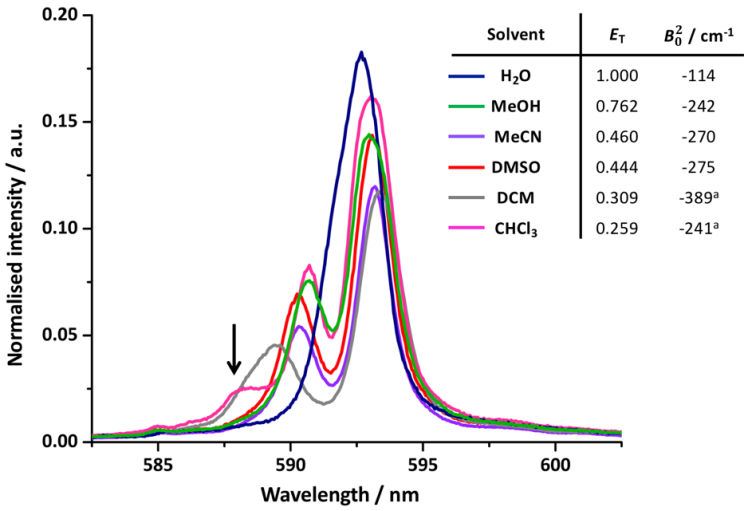

Fig. 3 Normalised emission spectra of [Eu.L^2] showing the ΔJ = 1 manifold in different solvents (295 K, λ_{exc} = 276 nm; slit widths: excitation 2.5 nm, emission 1.5 nm); the appearance of an additional emission band in $CHCl_3$ is highlighted. The Table shows calculated values of B_0^2 in each solvent. [a] Aggregated species in solution. Full emission spectra are given in Figure S4.

Solution Studies of [Ln.L^1] in Acidic Media

A logical progression of the initial work [5,7] with [Ln.L^1] was to extend the study on solvent effects to include the organic acids, acetic acid and trifluoroacetic acid, as hydrogen bond donor (HBD) solvents. [6] Whilst acetic acid is a weaker HBD than water or MeOH on the Kamlet-Taft $\propto$ scale,[16] trifluoroacetic acid provides one of

the strongest intermolecular hydrogen bonding interactions, owing to the electron withdrawing effect of the CF_3 group. The ^1H NMR spectrum of [Yb.L^1] in each solvent was analysed and proton longitudinal relaxation rates were measured to aid the full assignment of each ligand resonance. Comparative ^1H NMR spectral studies for [Yb.L^1] in five different solvents were thus undertaken to evaluate the effect of hydrogen bonding on NMR shifts, and hence deduce the magnetic susceptibility anisotropy behaviour.

With the exception of the three pyridyl protons, considerable line broadening and overlap of signals for [Yb.L^1] in CD_3COOD made it difficult to measure relaxation rates and assign ligand resonances with confidence, (Fig. 4). The NOESY spectrum of the analogous diamagnetic analogue [Y.L^1] in CD_3COOD and CF_3COOD revealed negative nOe's, while such effects were positive for [Y.L^1] in D_2O, CD_3OD and DMSO-d_6 , suggesting a change in the rate of molecular rotation (Figure S5).

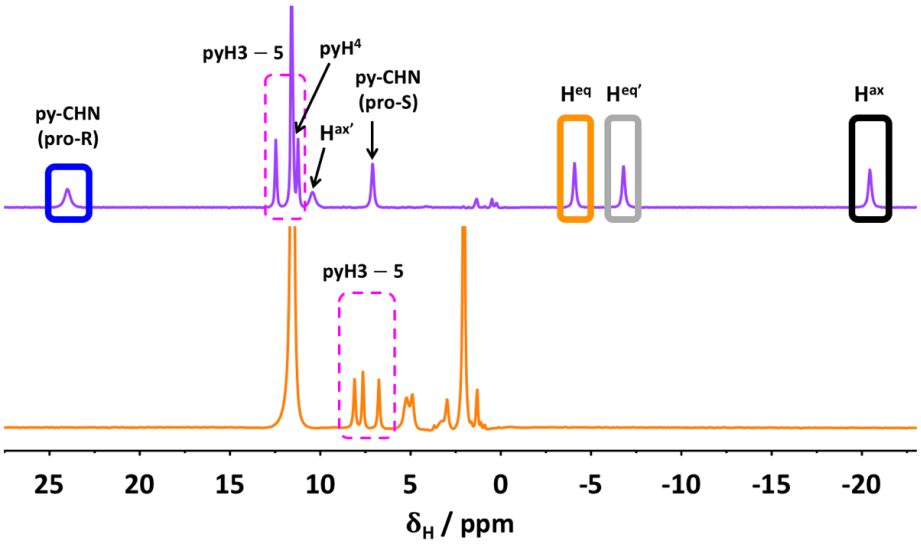

Fig. 4 Annotated ^1H NMR spectra of [Yb.L^1] in CF_3COOD (*purple*) and CD_3COOD (*orange*), showing the proton assignments (9.4 T, 295 K). The pyH^4 resonance in CF_3COOD overlaps with the solvent signal.

Comparative analyses of the experimental PCS of the pyridyl protons for [Yb.L^1] in the different solvents demonstrate a strong relationship between the solvent hydrogen bonding ability and PCS behaviour, (*Fig. 6*). Using calculations employed earlier in the analysis of [Yb.L^1] in D_2O, MeOD and DMSO-d_6,[6] the polar angle, θ, of the set of three O donor atoms in CF_3COOD was determined. Such an analysis requires determination of the magnetic susceptibility anisotropy in the relevant

solvent system. It can be found as the gradient in a plot of the experimental PCS of the ligand resonances versus their structural component term. Since the B_2^2 term is not present in a C_3 symmetric system, the anisotropy of the molar magnetic susceptibility ($\chi_{\parallel} - \chi_{\text{av}}$, where $\chi_{\text{av}} = \frac{(\chi_{\parallel} + 2\chi_{\perp})}{3}$) can be expressed as a ratio of the pseudocontact NMR shift (δ_{pc}) and a structural term $\left(\frac{3\cos^2\theta - 1}{r^3}\right)$, (Eq. 1).[6] Insufficient PCS data for **[Yb.L^1]** in CD_3COOD meant that a reliable linear fit to extract the magnetic anisotropy, ($\chi_{\parallel} - \chi_{\text{av}}$) could not be made, and consequently the polar angle of the O-donors, was not predicted.

$$\delta_{pc} = \frac{\chi_{\parallel} - \chi_{\text{av}}}{2N_A}\left(\frac{3\cos^2\theta - 1}{r^3}\right) \qquad (1)$$

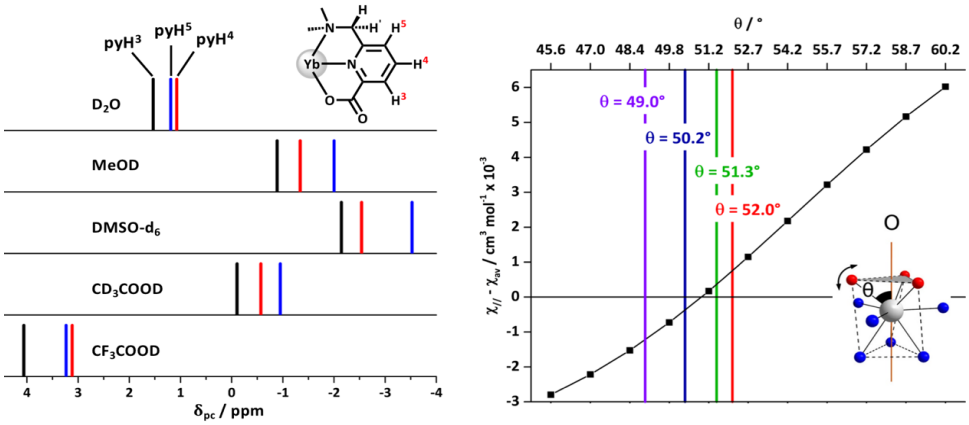

Fig. 6 Schematic representation of the pseudocontact shift of pyH$^{3-5}$ for [Yb.L^1] (9.4 T, 295 K) (*left*). Determination of the polar angle of the O donor atoms at which the calculated magnetic anisotropy (squares), extracted from variations in the polar angle of the O-donors from DFT optimised geometries in D_2O with imposed C_3 symmetry, matches the experimental anisotropy value found from PCS data analyses in DMSO-d_6 (*red*), CD_3OD (*green*), D_2O (*blue*), CF_3COOD (*purple*), (*right*).

The solvent dependence of the pseudocontact shift and, accordingly, the magnetic susceptibility anisotropy is evident on inspection of Figure 6. More importantly, there is an apparent change in the sign of the calculated room temperature anisotropy of the magnetic susceptibility on going from DMSO-d_6 and CD_3OD to D_2O and CF_3COOD, that was not observed for the Dy(III) analogue on varying the solvent. [6] Such behaviour highlights the hypersensitivity of the magnetic susceptibility anisotropy towards small perturbations in the geometric structure of the complex, i.e. $\Delta\theta = \pm 1.5°$ is sufficient for a sign change. The polar angle for the O donor atoms was found to be 49.0° in CF_3COOD, providing further evidence of a correlation between PCS behaviour, the hydrogen bonding ability of the solvent and the variation in the ligand polar angle. Thus, PCS of the pyridine protons becomes more positive as the oxygen donor atoms become more 'axial', due to a stronger hydrogen bonding effect involving the carboxylate oxygens. Whilst the observed PCS follows this general trend, the discrepancy in acetic acid is striking. It is a weaker HBD solvent than methanol and so its predicted PCS should be less positive. In this case, such behaviour can be tentatively ascribed to aggregation of the complex in CD_3COOD. Accordingly, DOSY-NMR spectra of [Y.L^1] were run in D_2O, CF_3CO_2D and CD_3CO_2D. The DOSY results show that the masses of the entities present in solution in CD_3CO_2D and in CF_3CO_2D are four and five times larger than those present in D_2O, (Table 2).

Table 2

Estimated molecular mass of [Y.L^1] in different solvents (center column) and the normalized ratio (right-hand column) with respect to the lowest figure. [a]

Solvent	MW_{est} / g mol^{-1}	Ratio
D_2O	369	1
CD_3COOD	1521	4
CF_3COOD	1941	5

a) Note how the estimated molecular mass of [Y.L^1] in D_2O is lower than the actual mass of the monomer. We attribute this underestimation to the fact that the molecular mass density ρ of these complexes is larger owing to the presence of the lanthanide atom, than the value estimated in reference 13. In spite of this deviation, it is very clear that [Y.L^1] aggregates (or self-organizes) in CD_3COOD and CF_3COOD.

Interactions between molecules in aggregates can cause significant changes to the coordination geometry and hence, perturb the magnetic susceptibility tensor to such an extent that the changes in PCS in CD_3COOD cannot be correlated with hydrogen bonding ability alone. It is also worth noting that in CF_3COOD, the appearance of other signals in the diamagnetic region of the ^1H NMR spectrum, although relatively small, signified the onset of acid-promoted decomplexation of the complex. Repeating the ^1H NMR experiments after two days saw an increase of the protonated ligand signals. It was hypothesised that protonation of the complex occurs at the carbonyl oxygen under these strongly acidic conditions, to generate the mono-cationic $[MLH]^+$ species, and it is this species that is observed in neat TFA solution.

To complement the ^1H NMR studies, further investigations with [Eu.L^1] using luminescence spectroscopy were conducted in CH_3COOH and CF_3COOH, in order to examine changes in spectral form and also deduce the B_0^2 parameter, representing the second-order crystal field term. The total emission spectrum in each solvent was recorded and the $^5D_0 \rightarrow {}^7F_1$ emission band was analysed in each case, (*Fig. 7*).

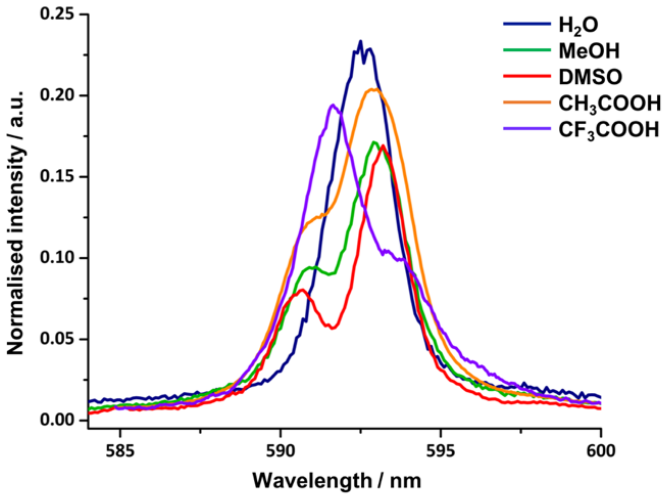

Fig. 7 The normalised emission spectra of [EuL^1] in the stated solvents showing the ΔJ = 1 manifold (295 K, λ_{exc} = 272 nm), highlighting the very different behaviour in CF_3COOH. Full spectra are given in Figure S6.

Comparative studies clearly show that the sign of B_0^2 is negative in each solvent except for CF_3COOH (+152 cm^{-1}) where it is positive and the degenerate doublet is higher in energy than the singlet. It is apparent that the $^7F_1$ splitting energy and hence B_0^2 is quite different in CH_3COOH (-170 cm^{-1}) and H_2O (-110 cm^{-1}).

Previous investigations have correlated the decrease in $|B_0^2|$ to decreasing values of θ.[6] Thus, the same type of structural sensitivity toward solvent change is observed by NMR and luminescence techniques. The unusual behaviour in acetic acid is highlighted once more, since the corresponding value of B_0^2 suggests a greater perturbation of the oxygen atoms towards axiality, notwithstanding the weaker HBD solvent donor ability of acetic acid, compared to MeOH.[16] Evidently, such behaviour may be attributed to the tendency to aggregate.

Summary and Conclusions

We have shown using a combination of emission spectra and NMR-diffusion measurements that the degree of aggregation of a lanthanide coordination complex can determine the ligand field. Such a conclusion adds further weight to refute the old dogma, still repeated in certain situations, that the optical emission spectra of lanthanide complexes are, to a good approximation, invariant with surroundings. Indeed, it is not just ligand constitution that determines the crystal field, notably the polarisability of the donor atoms and the ligand itself, but also the nature of the second sphere of coordination , primarily determined by solvent-complex and complex-complex interactions. Such work highlights the great scope that exists for creating NMR and optical spectral probes of the chemical environment with lanthanide complexes, but warns of the need to take care to calibrate the spectral response in the medium of the analyte.

We thank EPSRC for support EP/N006909/1. The authors declare no conflicts of interest.

Key Words Ligand field, europium, ytterbium, DOSY-NMR; paramagnetic shift.

References

1 O.A. Blackburn, R.M. Edkins, S. Faulkner, A.M. Kenwright, D. Parker, N.J. Rogers and S. Shuvaev, *Dalton Trans*. 2016, **45**, 6782.

2. M.C. Heffern, L.M. Matosziuk and T.J. Meade, *Chem. Rev*., 2014, **114**, 4496.

3. A.M. Funk, K.N.A. Finney, P. Harvey, A.M. Kenwright, E.R. Neil , N.J. Rogers, P.K Senanayake and D. Parker*, Chem. Sci*., 2015, **6**, 1655; G. Castro, M. Regueiro-Figueroa, D. Esteban-Gómez, P. Pérez-Lourido, C. Platas-Iglesias, and L. Valencia,

Inorg. Chem., 2016, **55**, 3490; K. L. N. A. Finney, A. C. Harnden, N. J. Rogers, P. K. Senanayake, A. M. Blamier, D. O'Hogain and D. Parker, *Chem. Eur-J*., 2017, **23**, 7976.

4. K. Binnemans, *Coord. Chem. Rev*. 2015, **295**, 1.

5. E. A. Suturina, K. Mason, C.F.G.C. Geraldes, I. Kuprov, D Parker, *Angew. Chem. Int. Ed*., 2017, **40**, 12215; O.A. Blackburn, N.F. Chilton, K Keller, C.E. Tait, W.K. Myers, E.J.L. McInnes, A M. Kenwright, P.D. Beer, C.R. Timmel, S. Faulkner, *Angew. Chem. Int. Ed*., 2015, **54**, 10783.

6. M. Vonci, K. Mason, E. A. Suturina, A. T. Frawley, S. G. Worswick, I. Kuprov, D. Parker, E. J. L. McInnes, and N. F. Chilton*, J. Am. Chem. Soc*., 2017, **139**, 14166.

7. K. Mason, A. C. Harnden, C. W. Patrick, A. W. J. Poh, A. S. Batsanov, E. A. Suturina, M. Vonci, E. J. L. McInnes, N. F. Chilton and D. Parker, *Chem. Commun*. 2018 submitted.

8. S.F. Mason, R.D. Peacock & B. Stewart, *Mol. Phys*., 1975, **30**, 1829; S.F. Mason*, Struct. Bonding*, 1980, **39,** 43.

9. M.F. Reid, F.S. Richardson, *Chem. Phys. Lett*. 1983, **95**, 5012.

10. G.S. Ofelt, J. Chem. Phys., 1962, **37**, 511; B.R. Judd, *Phys. Rev.*, 1962, 127, 750; C.K. Jorgensen and B.R. Judd, *Mol. Phys*., 1964, **8**, 281; R. Kuroda, S.F. Mason and C. Rosini, *J. Chem. Soc., Faraday Trans. 2*, 1981, **77**, 2125; F.S. Richardson, *Chem. Phys. Lett.,* 1982, **86**, 47.

11. C. S. Johnson Jr., *Prog. Nucl. Magn. Reson. Spectrosc.*, 1999, **34**, 203.

12. K. F. Morris, P. Stilbs and C. S. Johnson, *Anal. Chem.*, 1994, **66**, 211.

13. R. Evans, Z. Deng, A. K. Rogerson, A. S. McLachlan, J. J. Richards, M. Nilsson and G. A. Morris, *Angew. Chem. Int. Ed.*, 2013, **52**, 3199.

14. K. Binnemans and C. Görller-Walrand, *Chem. Phys. Lett.*, 1995, **245**, 75.

15. C. Reichardt, T. Welton, *'Solvents and Solvent Effects in Organic Chemistry*', C. Reichardt, T. Welton eds., Wiley-VCH, Weinheim, Germany, 2010, pp 425-508.

16. R. W. Taft and M. J. Kamlet, *J. Am. Chem. Soc.*, 1976, **98**, 2886.

17. S. Berger and S. Braun, *200 and More NMR Experiments*, Wiley-VCH, Weinheim, 2004.

TOC Graphic

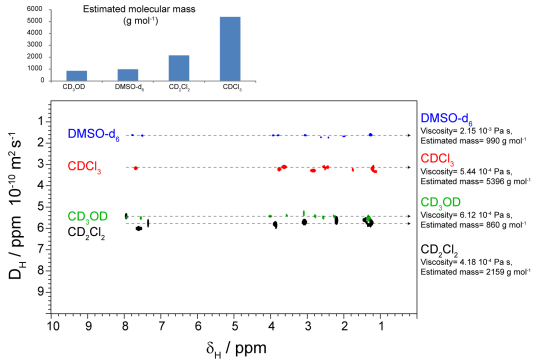
Estimated molecular mass
(g mol-1)
6000
5000
4000
3000
2000
1000
0
CD3OD
DMSO-d6
CD2Cl2
CDCl3
DMSO-d6
CDCl3
CD3OD
CD2Cl2
DMSO-d6
Viscosity= 2.15 10-3 Pa s,
Estimated mass= 990 g mol-1
CDCl3
Viscosity= 5.44 10-4 Pa s,
Estimated mass= 5396 g mol-1
CD3OD
Viscosity= 6.12 10-4 Pa s,
Estimated mass= 860 g mol-1
CD2Cl2
Viscosity= 4.18 10-4 Pa s,
Estimated mass= 2159 g mol-1
DH / ppm 10-10 m2 s-1
δH / ppm